Magnetic Anisotropy and Magnetization Dynamics of Individual Atoms and Clusters of Fe and Co on Pt(111)

T. Balashov,[1] T. Schuh,[1] A. F. Takács,[1,*] A. Ernst,[2] S. Ostanin,[2] J. Henk,[2] I. Mertig,[2,3] P. Bruno,[2,†] T. Miyamachi,[4]
S. Suga,[4] and W. Wulfhekel[1]

[1]*Physikalisches Institut, Universität Karlsruhe (TH), 76131 Karlsruhe, Germany*
[2]*Max-Planck-Institut für Mikrostrukturphysik, 06120 Halle, Germany*
[3]*Martin-Luther-Universität Halle-Wittenberg, Institut für Physik, 06099 Halle, Germany*
[4]*Graduate School of Engineering Science, Osaka University, Japan*
(Received 19 March 2009; published 25 June 2009)

The recently discovered giant magnetic anisotropy of single magnetic Co atoms raises the hope of magnetic storage in small clusters. We present a joint experimental and theoretical study of the magnetic anisotropy and the spin dynamics of Fe and Co atoms, dimers, and trimers on Pt(111). Giant anisotropies of individual atoms and clusters as well as lifetimes of the excited states were determined with inelastic scanning tunneling spectroscopy. The short lifetimes due to hybridization-induced electron-electron scattering oppose the magnetic stability provided by the magnetic anisotropies.

In modern magnetic recording, bits are stored in magnetically stable metallic grains, with larger densities being realized by reduced grain sizes. The magnetic stability is related to the grain's magnetic anisotropy energy (MAE) that has to be overcome to reverse the magnetization. Recently, a giant MAE of Co atoms on Pt(111) of 9.3 meV was found with x-ray magnetic circular dichroism (XMCD) [1]. This raised the hope for achieving the ultimate size limit in magnetically stable atoms or clusters at cryogenic temperatures. The challenge of studying magnetic stability lies in the direct investigation of a single atom, which is not possible by XMCD. We report here on the MAE and magnetization dynamics of single Fe and Co atoms and clusters on Pt(111) investigated with scanning tunneling microscopy (STM) and show that the quantum-mechanical nature of the magnetic system becomes essential.

To determine the MAE and the magnetization dynamics of individual atoms and small clusters, we performed inelastic tunneling spectroscopy (ITS) with a homebuilt low-temperature STM in ultrahigh vacuum. The tunneling electrons may exchange spin angular momentum with these magnetic objects [2]. The result of such inelastic spin-flip scattering is a change of the magnetization direction of the object [3]. For Fe and Co atoms and clusters on Pt(111) the uniaxial anisotropy dominates and favors perpendicular anisotropy [1,4]. In the quantum limit, i.e., for an isolated magnetic object with spin S, the uniaxial anisotropy energy can be written as DS_z^2 ($D < 0$ for easy axis out of plane). This description is linked to the classical uniaxial MAE $K\cos^2\theta$ by the correspondence principle $\cos\theta = S_z/S$ (θ is the angle of the magnetization with respect to the surface normal). To relate the spin-flip energy E_{sf} of a tunneling electron to the MAE, we note that upon spin-flip scattering the magnetic cluster is excited from its ground state with $S_z = \pm S$ to a state with

$S_z = \pm(S - 1)$, i.e., S_z of the object is changed by 1. For known S, K can be estimated as $E_{sf} \times S^2/(2S - 1)$ and $|D|(2S - 1) = E_{sf}$.

Inelastic spin-flip scattering shows up in ITS. ITS was so far restricted to atoms on insulating layers, e.g., Mn atoms on Al_2O_3 or CuN [2,5] but failed in entirely metallic systems. Recently, we have shown that even in metallic structures (bulk samples and thin films) spin-flip scattering can be detected [3,6,7]. Here we extend this technique to single atoms and clusters on Pt(111). In metallic systems, elastic tunneling leads to a linear dependence of the tunnel current I on the bias voltage U in the low bias regime. If $eU = E_{sf}$, an additional inelastic tunnel channel opens and the slope of $I(U)$ is increased for $eU > E_{sf}$. This change is usually too small to be identified directly. It can, however, be seen as a peak in d^2I/dU^2 [8,9]. The excitation occurs for both tunneling directions, with a dip appearing at negative bias.

To achieve a high surface quality, the Pt(111) substrate was cleaned by multiple cycles of Ar sputtering and annealing until contaminations were absent in STM images. W tips were cleaned in vacuum by flashing, such that the end of the tip melted. Small amounts (<0.01 atomic layer) of Fe or Co were deposited on Pt(111) at 4.3 K, resulting in isolated adatoms. d^2I/dU^2 spectra were recorded for Fe atoms and the Pt surface [crosses in Fig. 1(a)]. The second derivative was measured with a lock-in amplifier detecting the second harmonics in the tunnel current due to a 1.4–3.2 mV, 16.4 kHz modulated bias voltage. While spectrum (b) of the Fe atom on Pt(111) (see Fig. 1) clearly shows an "inelastic" minimum or maximum structure, the Pt spectrum (c) displays a minute signal. The genuine excitation spectrum (d) is obtained by subtracting (c) from (b) and is found to be almost symmetric, with the minimum and the maximum reflecting inelastic excitations. An excitation energy of ≈ 6 meV is estimated from a Gaussian fit
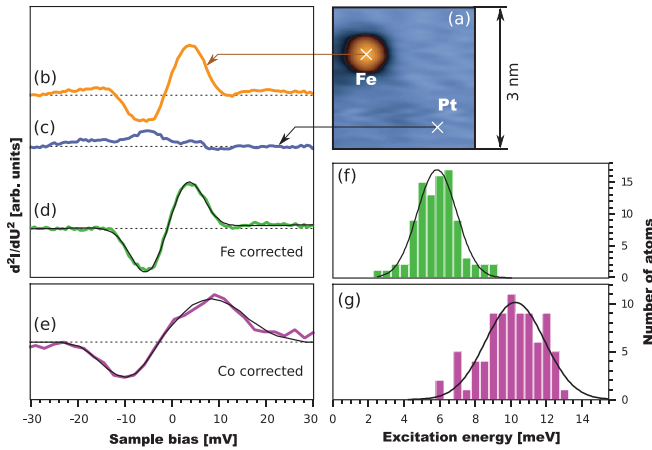
FIG. 1 (color).   (a) Topography of a single Fe atom on Pt(111).
(b) d^2I/dU^2 spectra of an Fe atom on Pt(111), (c) of the bare
Pt(111) background, and (d) the difference spectrum.
(e) Background-corrected Co spectrum. Gaussian fits are shown
in black. (f) Distributions of excitation energies for Fe atoms and
(g) for Co atoms.

of peak and dip. Co atoms on Pt(111) give very similar
results, providing ≈ 10 meV [see Fig. 1(e)].

The observed spectroscopic features are ascribed to
spin-flip excitations since other possibilities can be ex-
cluded as follows. (i) Plasmons in Fe, Co, and Pt have
energies in the range of several eV. Additionally, they
cannot be confined to single atoms, and therefore do not
explain the observed excitations. (ii) Atomic vibrations can
be excluded by first-principles calculations. The vibration
energies were obtained with the Vienna *ab initio* simula-
tion package (VASP) [10]. The potential landscape was
mapped by moving the adatom from its equilibrium posi-
tion in all directions. Within the harmonic approximation,
the softest phonon was estimated to 27 meV for Fe and
24 meV for Co. These energies are significantly larger than
the measured excitation energies. (iii) The Kondo effect
could produce similar features in the spectra [11].
However, Fe and Co on Pt(111) show no Kondo effect:
The perpendicular magnetic anisotropy of Co and Fe on
Pt(111) [1,4] lifts the spin degeneracy of the atom and
hinders the exchange of electrons with opposite spins
between the atom and the substrate [12,13]. Further, being
easily polarized, the magnetic moments at the Pt atoms
adjacent to the adatom [1,4,14] counteract the Kondo
screening. Thus, the observed inelastic features are clearly
attributed to magnetic excitations [15].

To determine the classical MAE from the excitation
energy, the spin S of the adsorbed atom and the induced
Pt moments must be known. We therefore calculated the
latter from first principles within our scalar-relativistic
Korringa-Kohn-Rostoker (KKR) approach. The large po-
larizability of Pt demands to treat an "extended impurity"
which comprises the adatom and five Pt layers with 16
Pt atoms each. The impurity is embedded in semi-infinite
Pt(111) by solving the Dyson equation for the Green func-

tion [16]. Exact positions of the Fe and Co adatoms, which
are crucial for calculating reliable electronic and magnetic
properties, are obtained by VASP [17,18]. The adatoms are
attracted by the surface, but the inward relaxation does not
strongly depend on the adsorption site (fcc of hcp).

The total spin magnetic moments (adatom and adjacent
Pt atoms) show an increase upon inward relaxation due to a
hybridization-induced polarization of Pt atoms while the
Co and Fe moments stay unchanged. A maximum at 25%–
30% of inward relaxation and a decrease upon further
inward relaxation is observed (see Fig. 2). The latter is
due to a decrease of the Fe and Co moments caused by
delocalization. Assuming bulk positions for the adatoms
results in significantly larger spin moments [1,4].

From the total spin magnetic moment of $2.2\mu_B$ for a
Co adatom in an fcc position we deduce $S = 1$, assuming a
Landé factor of $g \approx 2$. As a consequence, the excitation
energy from the ground state with $S_z = 1$ to the excited
state with $S_z = 0$ corresponds directly to the classical
uniaxial MAE [19].

The excitation energies were measured repeatedly [see
Fig. 1(g)]. The distribution fitted with a Gaussian yields an
average MAE of 10.25 meV per Co atom (cf. Table I). The
result agrees well with the experimental observations on an
ensemble of Co atoms using XMCD [1], thereby confirm-
ing our conclusion that the excitation is of magnetic origin.
A similar analysis was performed for Fe adatoms. The total
spin moment of $3.4\mu_B$ for fcc sites results in $S = 3/2$. The
Gaussian fit in Fig. 1(f) gives an average MAE of 6.53 meV
per Fe atom (see Table I).

Single adatoms can occupy fcc or hcp threefold hollow
sites on Pt(111). The potential barrier of ≈ 0.2 eV [20] for
hopping from an fcc to an hcp site hinders thermal diffu-
sion between the two positions at 4.3 K, suggesting that
adatoms occupy both sites equally likely. Interestingly, the
histograms for Fe and Co atoms are fitted well with a single
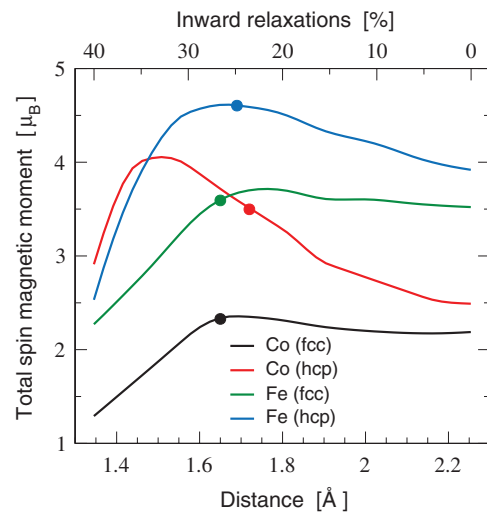

FIG. 2 (color).   Spin magnetic moments versus relaxation of
the Fe and Co adatoms. The circles indicate the equilibrium
distances.

TABLE I.   Measured excitation energies related to the MAE.

Cluster	Spin transition	Excitation energy [meV]	MAE [meV/atom]
Co_1	$1 \rightarrow 0$	10.25 ± 0.15	10.25 ± 0.15
Co_2	$2 \rightarrow 1$	8.2 ± 0.4	5.5 ± 0.3
Co_3	$3 \rightarrow 2$	8.3 ± 1.2	5.0 ± 0.8
Fe_1	$3/2 \rightarrow 1/2$	5.83 ± 0.08	6.53 ± 0.09
Fe_2	$3 \rightarrow 2$	5.98 ± 0.09	5.20 ± 0.09
Fe_3	$9/2 \rightarrow 7/2$	6.5 ± 0.2	5.5 ± 0.2

Gaussian. This observation implies that either the excitation energies do not vary with position (within the resolution of ≈3 meV) or that only one of the two positions is occupied.

To corroborate the experiment we computed MAEs using our relativistic layer-KKR code, invoking the magnetic force theorem [21]. The MAE of a relaxed Fe atom is approximately 3.2 meV in fcc and 0.4 meV in hcp positions; for a Co atom we find 3.1 meV for fcc and 3.8 meV for hcp positions. These values are smaller than the experimental ones but of the same order of magnitude. The MAE for Fe in the hcp position is significantly smaller than the experimental value, suggesting that Fe in the fcc position is mainly probed: Because of large tunnel currents, the adatoms are possibly moved to the more stable fcc sites. In the case of Co, there is no significant difference in MAE on the hcp and fcc sites. The agreement with experiment is substantially better for Fe than for Co, pointing to the importance of correlation effects in systems with localized $3d$ electrons that are not fully treated within the local spin density approximation (LSDA). The additional d electron of Co with respect to Fe causes stronger correlations and requires to go beyond LSDA.

The probability of spin-flip scattering, as determined from the area under the inelastic peaks, is ≈2% for both Fe and Co if the bias energy exceeds the MAE. This implies that at high bias even with tunnel currents in the pA range, the magnetic state of the atoms is flipped at a rate too high to be observed in STM. This explains the absence of the hysteresis for single Co atoms recently found at a sample bias of ≈200 mV [22]. Note also that the peaks in the spectra are rather broad, an effect accounted for by short lifetimes but not by thermal smearing or the lock-in modulation. Having corrected for experimental broadening [9], the widths of the inelastic peaks of Fe and Co are 5.6 and 18 meV, respectively, which correspond to lifetimes of the excited states of less than 60 fs for Fe and 24 fs for Co atoms. These lifetimes are shorter than the time between consecutive spin-flip events (≈0.5 ns at $I \approx 10$ nA with 2% scattering probability). Therefore only excitations from the ground state are observed.

Lifetimes provide information on the magnetization dynamics which is not accessible by XMCD. The above lifetimes indicate efficient relaxation processes which are absent for magnetic ions in insulators [5]. Since comparable MAEs were found in metals and insulators, spin-orbit interaction can be ruled out as a relaxation mechanism. More likely, the strong hybridization of the adatom states with those of the Pt substrate leads to efficient electron-electron scattering processes that relax the magnetic state of the adatom: The smaller hybridization of the Fe-$3d$ states with the Pt-$5d$ states as compared to Co leads to both a lower MAE and to a longer lifetime of the excited Fe state than that of Co.

Using the atomic manipulation capabilities of the STM [23], it is possible to extend the investigation to well-defined Fe and Co clusters composed of two and more atoms [here, dimers and trimers; Fig. 3(a)]. The dimers—and even more trimers—appear significantly higher than single atoms in topographic scans [Fig. 3(b); cf. Ref. [24]].

To investigate the inelastic excitations of clusters we use the same approach as for single atoms. In Fe and Co clusters the local magnetic moments couple ferromagnetically, and the total spin of the cluster is obtained by adding individual spins. There are, however, two different types of spin-flip excitations in clusters, as illustrated by a low- and a high-energy excitation in the dimer spectrum in Fig. 3(c).

(i) At low energies, the magnetic moment of the entire cluster can be rotated collinearly, i.e., the total spin S of the cluster is rotated but its length stays constant. In analogy to single atoms we obtain the MAE of the cluster from this excitation energy (see Table I). In agreement with XMCD data and calculations [1], the MAE per atom drops with the size of the cluster. This is due to quenching of the orbital moment. While a single adatom on Pt(111) has a high rotational symmetry with respect to rotation about the surface normal, this symmetry is broken with adding another atom. The third atom lowers the MAE only slightly. The experiment shows that such a tendency does not depend on the adatom species. The MAEs of Co trimers agree as well with XMCD data.

(ii) At higher energies, the "inner" magnetic structure of the cluster can be excited into a noncollinear state. In addition to the anisotropy energy, exchange energy has to be paid, being typically 1 order of magnitude larger. High-energy excitations appear in experiment as broad peaks around 50 meV for Fe dimers (Fig. 3(c)). The width of 33 meV is caused by the short lifetime of the excited state (≈10 fs). An evaluation of 18 dimers gives an excitation energy of 54 ± 2 meV. Assuming a spin of $S = 3$ for the Fe dimer, the quantum-mechanical excitation energy is $3J + 5|D|$. With $|D| = 1.15 \pm 0.02$ meV, obtained from the first excitation, this gives an exchange constant J of 16 ± 1 meV. The extremely short lifetime of the noncollinear state is due to the exchange interaction. This interaction conserves S_z but may alter S, so that a noncollinear state can rapidly decay into a collinear excited state with identical S_z. To elucidate this experimental finding we estimated the exchange energy of a Fe dimer on Pt(111) from first-principles calculations. The least-energy configuration is a dimer with Fe atoms occupying next-nearest
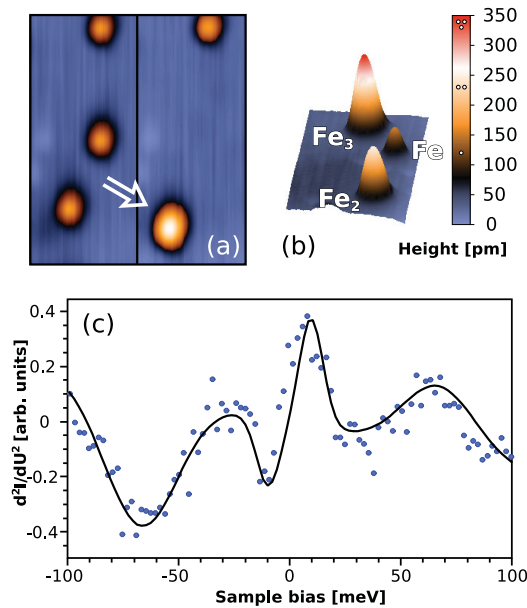
FIG. 3 (color). (a) Formation of a Co dimer by manipulating two Co atoms by the STM (arrow). (b) 3D view of an Fe atom, dimer, and trimer. (c) d^2I/dU^2 spectra of an Fe dimer on Pt(111) with two excitations visible. Gaussian fits are shown as solid line.

neighbor fcc and hcp positions. The magnetic moments of $2.85\mu_B$ per atom align parallelly and the exchange constant J is estimated to 11 meV, in a reasonable agreement with experiment. The theoretical value is lower than the experimental one, most likely due to the limited treatment of correlations in LSDA.

The classical MAE found for individual Fe and Co adatoms and clusters predicts stable magnetic configurations on the time scale of years at temperatures below 2 K. When treating the cluster as a quantum-mechanical system, tunneling between magnetic states has to be considered [25]. The magnetization tunneling is induced either by a transversal magnetic field (absent in our studies) or by an in-plane anisotropy. The threefold-rotational symmetry of the substrate results in MAE terms of at least sixth order which contribute only for $S \geq 3$ [26] and can thus be excluded for Fe and Co. An additional mechanism for spin reversal is, however, provided by the electron-electron interaction. Hybridization of the adatom states with those of the Pt substrate leads to short lifetimes and increased energy smearing of the excited state. Thus, an overlap of the ground state and the excited state is likely despite the large MAEs. It results in a nonzero transition probability between the degenerate ground states via an intermediate excited state.

In conclusion, the magnetic stability of atoms and small clusters is related to the hybridization in two opposing ways. On one hand, the hybridization increases the anisotropy, stabilizing the spin. On the other hand, it decreases the lifetime of the excited state, destabilizing the spin.

Only by decoupling these effects, magnetically stable atoms and clusters may be realized. The presented ITS approach will help to find the best combination of magnetic atoms and substrates to achieve this goal.

Note added in proof.—A theoretical description of the scattering process was recently published [27].

*Present address: Faculty of Physics, Babes-Bolyai University, 400084 Cluj-Napoca, Romania.
†Present address: European Synchrotron Radiation Facility, 38043 Grenoble Cedex, France.
[1] P. Gambardella *et al.*, Science **300**, 1130 (2003).
[2] A. J. Heinrich *et al.*, Science **306**, 466 (2004).
[3] T. Balashov *et al.*, Phys. Rev. B **78**, 174404 (2008).
[4] C. Etz *et al.*, Phys. Rev. B **77**, 184425 (2008).
[5] C. F. Hirjibehedin *et al.*, Science **317**, 1199 (2007).
[6] T. Balashov, A. F. Takács, W. Wulfhekel, and J. Kirschner, Phys. Rev. Lett. **97**, 187201 (2006).
[7] C. L. Gao *et al.*, Phys. Rev. Lett. **101**, 167201 (2008).
[8] E. L. Wolf, *Principles of Electron Tunneling Spectroscopy* (Oxford University, New York, 1985).
[9] B. C. Stipe, M. A. Razaei, and W. Ho, Science **280**, 1732 (1998).
[10] G. Kresse and J. Furthmüller, Phys. Rev. B **54**, 11 169 (1996).
[11] N. Knorr *et al.*, Phys. Rev. Lett. **88**, 096804 (2002).
[12] M. N. Leuenberger and E. R. Mucciolo, Phys. Rev. Lett. **97**, 126601 (2006).
[13] A. F. Otte *et al.*, Nature Phys. **4**, 847 (2008).
[14] T. Herrmannsdoerfer, S. Rehmann, W. Wendler, and F. Pobell, J. Low Temp. Phys. **104**, 49 (1996).
[15] Note that magnetic excitation arises in different spin channels depending on the tunneling direction leading to slightly asymmetric intensities above and below E_F [3].
[16] K. Wildberger *et al.*, Phys. Rev. Lett. **75**, 509 (1995).
[17] R. F. Sabiryanov *et al.*, Phys. Rev. B **67**, 125412 (2003).
[18] A. Mosca Conte, S. Fabris, and S. Baroni, Phys. Rev. B **78**, 014416 (2008).
[19] By considering the impurity as a quantum spin with half-integer spin, hybridization with the substrate is neglected. Treating the hybridization would require an itinerant treatment of the impurity.
[20] M. Ternes *et al.*, Science **319**, 1066 (2008).
[21] X. Wang *et al.*, J. Magn. Magn. Mater. **159**, 337 (1996).
[22] F. Meier *et al.*, Science **320**, 82 (2008).
[23] D. M. Eigler and E. K. Schweizer, Nature (London) **344**, 524 (1990).
[24] W. Chen, T. Jamneala, V. Madhavan, and M. F. Crommie, Phys. Rev. B **60**, R8529 (1999).
[25] S. Bertaina *et al.*, Nature (London) **453**, 203 (2008).
[26] Note that a sixfold in-plane anisotropy is proportional to $(\hat{S}_+^6 + \hat{S}_-^6)$ and thus vanishes if $S < 3$. $\hat{S}_+$ and $\hat{S}_-$ are the spin "ladder" operators.
[27] J. Fransson, Nano Lett. **9**, 2414 (2009).